PROTEINS: Structure, Function, and Bioinformatics 59:240–251 (2005)

Comparative Structural Analysis of TonB-Dependent Outer Membrane Transporters: Implications for the Transport Cycle

David P. Chimento,[1] Robert J. Kadner,[1] and Michael C. Wiener[2]*
[1]*Department of Microbiology, University of Virginia, Charlottesville, Virginia*
[2]*Department of Molecular Physiology and Biological Physics, University of Virginia, Charlottesville, Virginia*

ABSTRACT **TonB-dependent outer membrane transporters (TBDTs) transport organometallic substrates across the outer membranes of Gram-negative bacteria. Currently, structures of four different TBDTs have been determined by X-ray crystallography. TBDT structures consist of a 22-stranded β-barrel enclosing a hatch domain. Structure-based sequence alignment of these four TBDTs indicates the presence of highly conserved motifs in both the hatch and barrel domains. The conserved motifs of the two domains are always in close proximity to each other and interact. We analyzed the very large interfaces between the barrel and hatch domains of TBDTs and compared their properties to those of other protein–protein interfaces. These interfaces are extensively hydrated. Most of the interfacial waters form hydrogen bonds to either the barrel or the hatch domain, with the remainder functioning as bridging waters in the interface. The hatch/barrel interfacial properties most resemble those of obligate transient protein complexes, suggesting that the interface is conducive to conformational change and/or movement of the hatch within the barrel. These results indicate that TBDTs can readily accommodate substantial conformational change and movement of their hatch domains during the active transport cycle. Also, these structural changes may require only modest forces exerted by the energy-coupling TonB protein upon the transporter. Proteins 2005;59:240–251.**

Key words: BtuB; FepA; FhuA; FecA; Vitamin B_{12}; cobalamin; membrane proteins

INTRODUCTION

The outer membrane is an essential component of Gram-negative bacteria, providing them with increased resistance to antibiotics, digestive enzymes, detergents and immune surveillance.[1] Gram-negative bacterial outer membrane transporters include proteins that form transmembrane pores and transport relatively large organometallic molecules (≥600 Da) from the external milieu into the periplasm in an energy-dependent process. Outer membrane active transporters bind ligands with high affinity and specificity in an energy-independent step, but transport of their cognate substrates requires the cytoplasmic membrane-associated TonB–ExbB–ExbD complex. TonB is a three-domain protein containing an amino-terminal (putative) transmembrane helix that anchors the protein in the cytoplasmic membrane, a central proline-rich domain that resides within the periplasm, and a carboxy-terminal globular domain that is also in the periplasm. ExbB and ExbD reside within the cytoplasmic membrane, associate with TonB, and are necessary for full TonB function.[2,3] The coupling of TonB to the TonB-dependent outer membrane transporter (TBDT) is essential for the active transport cycle. The mechanism of energy transduction from the cytoplasmic (inner) membrane to the TBDT is currently not well understood.[4,5]

TBDTs possess a conserved sequence, the 'Ton-box,'[6,7] that interacts with the TonB protein. Currently accepted models of TBDT function entail a substrate-binding event and an energized transport step that is dependent upon TonB. After the substrate binds to the TBDT, the Ton-box changes its relative position and becomes accessible for interaction with TonB.[8–13] Most mutations in the Ton-box have little effect on the function of BtuB or FecA except for proline or glycine substitutions at the Ton-box +3 or +6 positions, suggesting that the interaction with TonB does not depend upon the type of side chain in the Ton-box.[4,13] The stoichiometry of TonB and its interaction with TBDTs are complex. Variable-length deletion constructs of TonB, lacking the N-terminal membrane anchor, exist in both monomeric and dimeric forms; both are able to interact with FhuA.[14,15] Constructs containing most but not all of the TonB C-terminal domain dimerize both in solution and in crystal structures.[15,16] In addition to the C-terminal domain that binds to the Ton-box of TBDTs, a second interaction site outside of the TonB C-terminal domain has been observed.[14,17] The affinity of TonB for TBDTs in vitro

Abbreviations: TBDT, TonB-dependent outer membrane transporter.

This work was supported by National Institutes of Health Grants GM019078 (D.P.C and R.J.K.) and DK59999 (D.P.C. and M.C.W.).

David P. Chimento's present address is the Department of Physiology, University of Pennsylvania School of Medicine, D501, Richards Laboratory, Philadelphia, PA 19104

*Correspondence to: Michael C. Wiener, Department of Molecular Physiology and Biological Physics, University of Virginia, Charlottesville, VA 22908-0736. E-mail: mwiener@virginia.edu.

Received 21 August 2004; Revised 11 November 2004; Accepted 12 November 2004

Published online 28 February 2005 in Wiley InterScience (www.interscience.wiley.com). DOI: 10.1002/prot.20416

can be modulated by the presence of substrate, and one or two TonB proteins can bind to the TBDT.[14,15]

Currently, crystal structures of four TBDTs are available: FhuA,[12,18] FepA,[19] FecA,[20,21] and BtuB.[22] Each TBDT structure is composed of two domains, a conserved N-terminal globular domain (hatch) and a 22-stranded β-barrel (barrel) (Fig. 1). Both the hatch and barrel domains are unique; neither structure is present in any proteins except TBDTs. These TBDT crystal structures are conformations of substrate-free and substrate-bound energy-independent states of the transport cycle. The substrates are bound in the lumen at the extracellular face by residues of both the hatch and the barrel. Conformational changes occur in both the hatch and barrel loops to form intimate contact with substrate, leading to high-affinity binding.[12,18–20,22] In all TBDT structures determined to date, the hatch rests within the barrel and occludes the large (≈35–40 Å diameter) pore of the barrel. The presence of the pore-occluding hatch strongly suggests that a conformational change must occur in TBDTs to allow passage of their substrates (which have masses of 500–1400 Da) across the outer membrane. One of the most distinctive general features of TBDTs is the very large interface between the hatch and barrel domains. The ordered regions of hatch domains observed in TBDT structures are 131–142 amino acids in length (14100–15477 Da in molecular weight); these domains make numerous interactions with the barrel across the interface.

We have performed a series of structural analyses of the four TBDT structures solved to date. The use of structural information powerfully augments sequence alignment and permits the identification of short sequence patterns possessing invariant structural features. Nearly all of these conserved structural motifs occur at the hatch–barrel interface. We characterized the properties of the hatch–barrel interfaces of TBDTs; this characterization included an examination of the crystallographic waters present in the refined structures. These interface properties are similar to those observed in the interfaces of transient protein complexes in which substantial conformational changes between domains is required for function. These analyses strongly support the hypothesis that substantial conformational change occurs during the active transport cycle of TBDTs in order to permit substrate to traverse through the barrel. Additionally, our analysis suggests qualitatively that there is minimal energetic cost to perturb the hatch–barrel interface during the transport cycle. Movement and/or conformational change of the hatch domain will change its interface with the barrel; this change can be readily accommodated by solvating waters with excess hydrogen-bonding capacity that are already present in the interfacial region.

MATERIALS AND METHODS

The structures of BtuB[22] (1NQE), FepA[19] (1FEP), FhuA[12,18] (1QFG), FecA[20] (1KMO) were aligned using the K2[23] automated alignment server (http://zlab.bu.edu/k2/index.shtml). To produce the structure-based sequence alignment, the protein sequences of TBDT were aligned using CLUSTALW.[24] BIOEDIT was then used for manual editing of the sequence alignment to reflect structural information.[25]

The interfacial surface area, the area that becomes inaccessible to solvent due to the hatch–barrel interaction, was determined using the program NACCESS[26] with a probe size of 1.4 Å. The change in the interfacial accessible surface area (ΔASA) was calculated as half of the sum of the total ΔASA for both domains in the complex. The hydrogen bonding profile between the hatch and barrel domains was determined using the programs DIMPLOT[26] and HBPLUS.[27] The accessible surface area of the hatch domain was determined using NACCESS as stated above. The fractional surface area of the hatch domain that is covered by water was calculated as $(ASA_{HATCHdry} - ASA_{HATCHwet})/ASA_{HATCHdry}$, where $ASA_{HATCHwet}$ is the ASA of the hatch domain with crystallographic waters included, and $ASA_{HATCHdry}$ is the ASA of the hatch with the waters omitted. The expected volume of a protein is approximated by $V \approx 1.27\, M_w$ Å^{3*} dalton^{-1}.[28] The number of hydrogen bonds per interface was calculated as one-half the number of H-bonds divided by the interfacial accessible surface area. Salt bridges were defined as donor residues lysine, arginine, and histidine at a distance less than 4 Å from acceptor residues aspartic acid or glutamic acid. The electrostatic surfaces of the hatch and barrel domains were determined using the electrostatic surface calculation function in GRASP.[29] The shape correlation statistic S_c was calculated with the SC program of the CCP4 suite.[30] Gap index was defined as follows: gap index (Å) = gap volume (Å^3)/interface ASA (Å^2).[31] Figures 1, 4–9, and 10(b) were made with PYMOL.[32]

RESULTS AND DISCUSSION

Structure-Based Sequence Alignments Reveal Highly Conserved Motifs

The sequences of the four TBDTs were aligned based upon their substrate-free (apo-) structures (Fig. 2). In pairwise alignment, the TBDT sequences have an identity of 16–23%; in a multiple sequence alignment, the identity is only ≈5%. The majority of identity is in the hatch domain, with nine highly conserved sequence motifs. Overall, the β-barrel is poorly conserved in sequence; some residues are identical in periplasmic turns and in strands β9 through β18. Although rows of aromatic residues reside at the positions of the membrane interfaces, this structural feature is not readily noticeable in the sequence alignment. Our initial structure-based alignment was compared to other TBDTs from *E. coli* and from distantly related Gram-negative bacterial species. The set included TBDTs that transported six different substrates: cobalamin, ferric enterobactin, ferrichrome, ferric dicitrate, ferric catechol, and heme. For each substrate, two transporters were included, one from *E. coli* and the other from a different Gram-negative bacterium. The results of this sequence alignment indicate that motifs conserved among

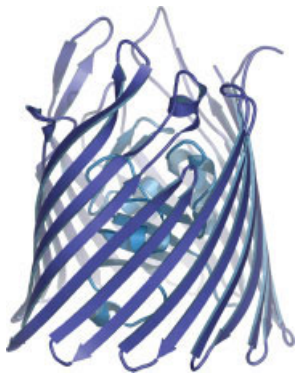

Fig. 1. Ribbon diagram of BtuB, a TBDT. TonB-dependent transporters possess two domains, a 22-stranded anti-parallel β-barrel (barrel), and an N-terminal domain (hatch) that resides within the barrel. The β-strands of the barrel are connected on the periplasmic side by short turns and on the extracellular side by long flexible loops.

the four TBDTs of known structure are also highly conserved among more distantly related bacterial TBDTs (data not shown).

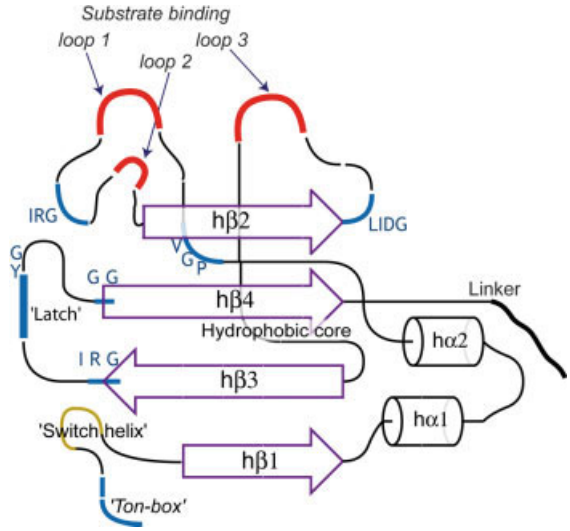

Fig. 3. Two-dimensional schematic of the N-terminal domain of TBDTs. The conserved features of the general fold are shown: β-strands as rectangular arrows, α-helices as cylinders, loops as thin lines. Conserved motifs of currently unknown function are labeled in blue. Substrate binding loops are shown in red, and the hatch–barrel linker is shown in black. The 'switch-helix,' found only in the FecA and FhuA structures, is shown in yellow.

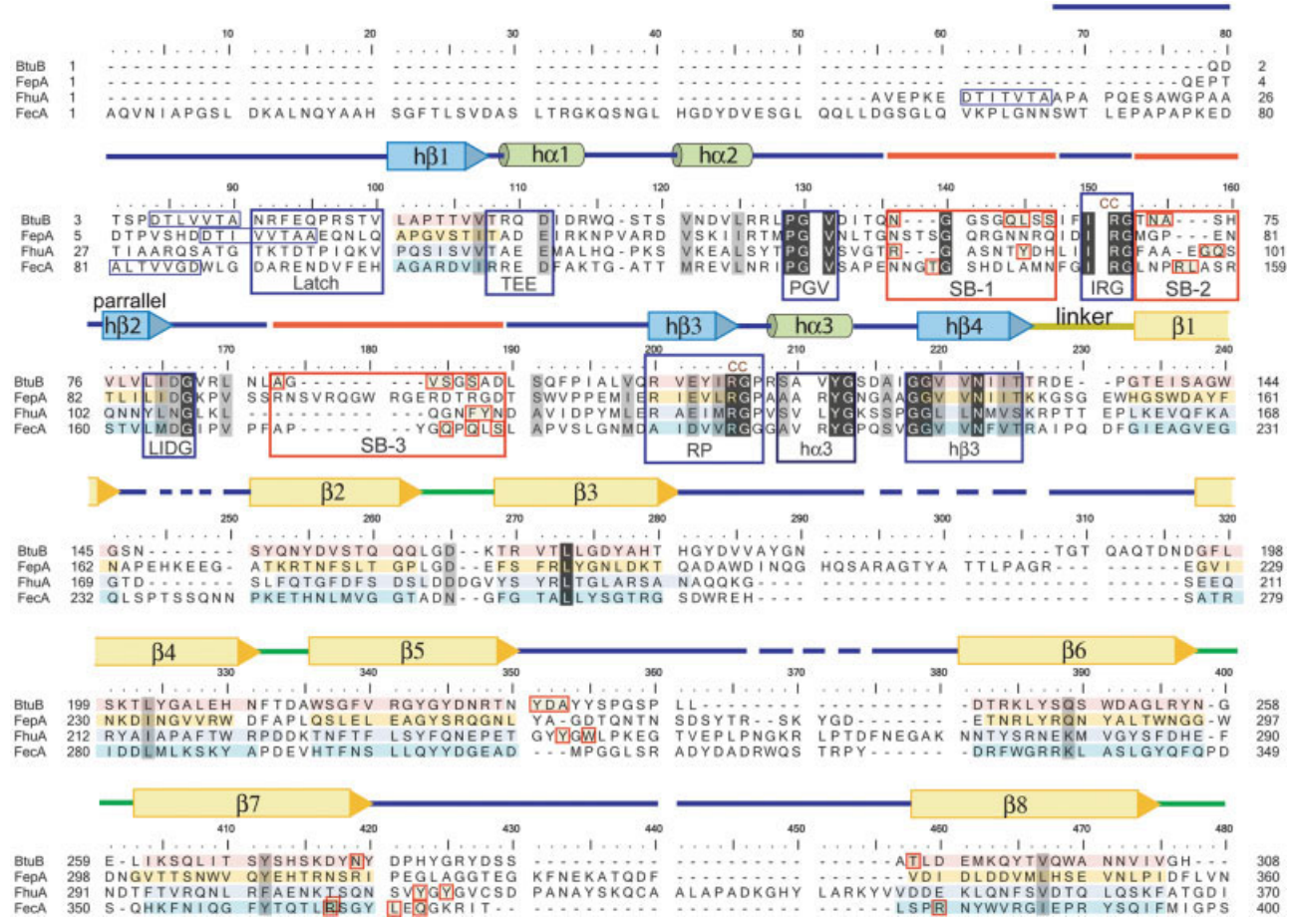

Fig. 2. Structure-based sequence alignment of BtuB, FepA, FhuA and FecA. Secondary structure elements are indicated above the sequence. Lines indicate loops of the hatch and barrel domains (blue is any loop, and green indicates a periplasmic turn of the barrel); loops and turns are *L* and *T* respectively; boxes indicate β-strands (blue is in the hatch, yellow is in the barrel); cylinders indicate α-helices. Conserved sequence features are indicated by open boxes around the sequence; open blue boxes indicate conserved sequence elements with currently undefined functional roles; open red boxes refer to substrate-binding motifs and to specific substrate binding residues. The brief text below the sequence is the motif identifier and corresponds to descriptions in Figure 3, in Tables III and IV, and in the text. The uppercase CC found in four locations indicates residues that are located in the conserved charge cluster described in the text.

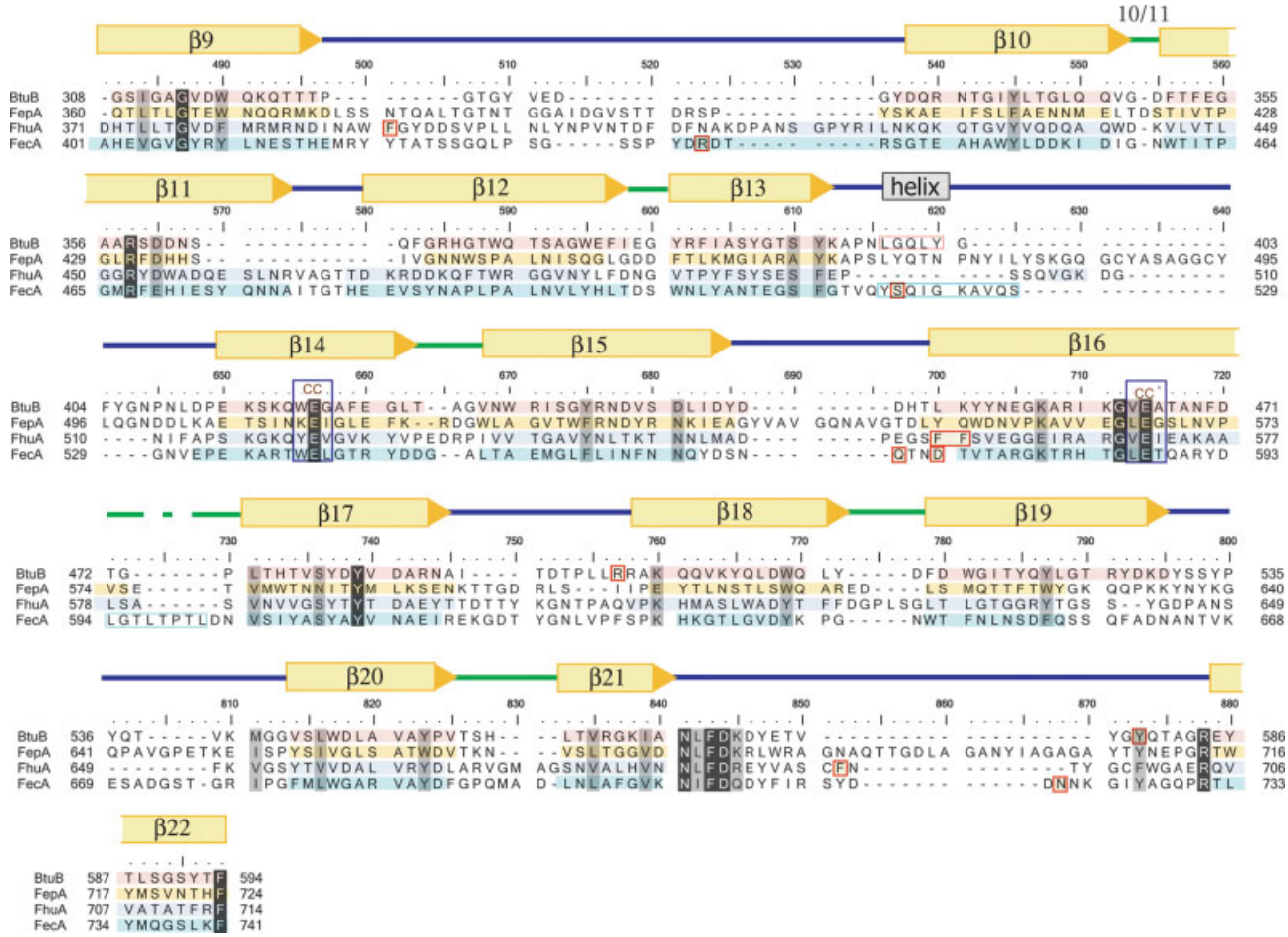

Figure 2. (Continued.)

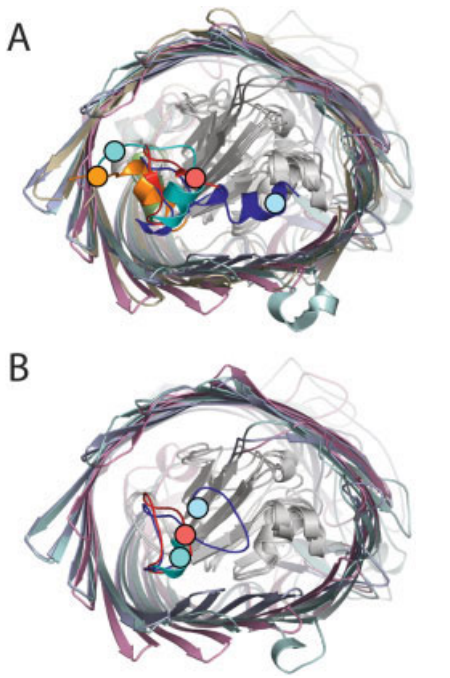

Fig. 4. Position of the Ton-box before and after substrate binding. (**A**) The substrate-free form of the periplasmic opening of BtuB (pink), FepA (orange), FhuA (blue), and FecA (cyan). (**B**) The substrate-bound form of the periplasmic opening. The experimentally determined or inferred position of the Ton-box (see text) is shown for each TBDT by a circle.

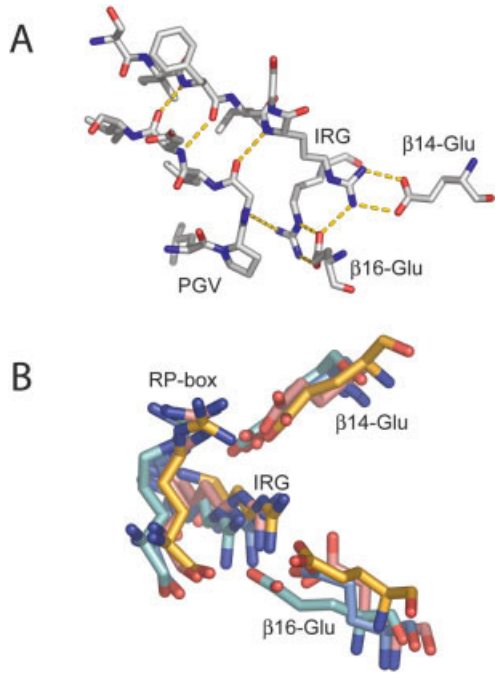

Fig. 5. Conserved PGV-IRG and charge cluster motifs. (**A**) Conserved hydrogen bonding of substrate-binding loops SB1 and SB2 near the charge-cluster of BtuB. (**B**) Charge cluster in structures of TBDTs. The locations of conserved features are labeled according to the text. Two arginines from the N-terminal domain are on the left and two glutamates from the β-barrel are on the right side in the figure. Shown are BtuB (pink), FepA (orange), FhuA (blue), and FecA (cyan).

Hatch Domain Contains Conserved Structural Motifs

Nine hatch domain regions, conserved in both sequence and structure, are listed in Table I and shown schematically in Figure 3. The amphipathic helices hα1 and hα2 interact with the core β-strands through their hydrophobic faces. The C_α backbones of the hatch domains align with an RMSD of 1.25 Å. The hatch domain structures are nearly identical in the β-strand core with larger variation in substrate binding loops (apices) and N-termini. The highly conserved N-terminal Ton-box motif is located at the periplasmic opening of the barrel of TBDTs, shown in Figure 4(a). The position of the Ton-box is in a different relative position among all four TBDT structures. The sequences located N-terminal of the Ton-box vary in length among TBDTs. Some TBDTs possess a long N-terminal extension that functions as a transcriptional regulatory domain.[33] The FecA N-terminal extension is 79 residues long, but in TBDTs lacking this regulatory domain the extension is 5–15 residues in length.[34]

With the exception of FepA, three TBDT structures exist in both substrate-free (apo-) and substrate-bound forms. The Ton-box position changes upon substrate binding in each of these three TBDTs [Fig. 4(b)]. Within the hatch, FecA and FhuA have a structurally defined motif called the 'switch-helix.'[12] The switch-helix is between the Ton-box and hβ1. This switch-helix is observed to unwind upon substrate binding in FhuA and FecA, moving the Ton-box by as much as 20 Å.[12,20] The large displacement of the end of the switch helix observed upon its substrate-induced unfolding in FhuA and FecA strongly suggests that the structurally disordered Ton-box would be extended away from the hatch core into the periplasmic space. However, FepA and BtuB lack this switch helix motif, and removal of the switch-helix conferred only modest reduction in transport activity in FhuA.[35] The crystal structure of the substrate-bound form of BtuB shows a movement of several residues in the Ton-box and a disordering of the Ton-box residues (e.g., increased relative B-factors compared to those of the apo-structure); however, the residues of the Ton-box are discernible in the electron density. Electron paramagnetic resonance (EPR)[11,36] and biotin labeling[9] experiments indicate an order-to-disorder transition upon substrate binding. A more recent EPR study[37] compared the effects of various solutions upon spectra obtained from BtuB. High-osmolarity solutions, such as those used in the crystallization of BtuB,[38] inhibited the disordering seen in 'standard' low-osmolarity solutions. Therefore, three Ton-box conformations in BtuB have been observed (or inferred, in the case of EPR and biotin labeling): an ordered conformation in the absence of substrate, an ordered but shifted conformation in the presence of substrate (which may be an intermediate conformation), and a disordered 'signaling' conformation in the presence of substrate.

Substrate-Binding Loops (Apices) of TBDT Hatch Domains Are in Similar Spatial Locations and Are Flanked By Highly Conserved Sequences

Three apical loops of the hatch form the lower portion of the TBDT substrate-binding site (Fig. 3). The common position of these apical hatch loops is maintained by conserved turns in the hatch and by local charge interactions between the hatch and barrel. Two of the most strictly conserved sequences in TBDT are the PGV and IRG motifs (Table I). The conservation of these sequences was noted previously when several TBDT genes were sequenced[6,39] and also in a previous structure-based sequence alignment.[21] The PGV and IRG sequences flank substrate-binding loops 1 and 2. Figure 5(a) shows the positions of PGV and IRG relative to the substrate binding loops. The PGV motif is a sharp turn in the hatch leading to formation of the apical loop that is substrate-binding site 1 (SB1). Terminating the SB1 loop is the IRG sequence. Although the SB1 sequences are not conserved, multiple structure alignment reveals a common position for the SB1 loop proximal to barrel strands β4, β21, and β22. Like PGV, the IRG motif is also a sharp turn producing the second substrate-binding motif 2 (SB2). The IRG motif is 'locked' into position by electrostatic interactions in a multiple-charge cluster of two arginines and two glutamates. The PGV motif is positioned adjacently to the IRG motif through four hydrogen bonds to the IRG backbone. The RP-box, part of hβ3, contributes the second arginine. The charge cluster is completed by two conserved glutamates contributed by barrel strands β14 and β16 [Table I, Fig. 5(b)]. Each TBDT structure is slightly different in the geometry of the interactions in the charge cluster. The Arg and Glu residues may be in position to form salt bridges, hydrogen bonds, or both. Mutagenesis of this charge cluster affects TBDT function, although the specific role of this structural motif is unclear.[35,40,41] Substrate binding site 3 (SB3) is formed beginning with the highly conserved LIDG-motif of hβ2. SB2 and SB3 lack sequence conservation (Fig. 2), but as for SB1 structure alignment shows a common spatial location for both loops within the aligned structures. The substrate-binding site of FepA is unknown; thus we infer FepA SB1–SB3 by homology in our alignments. In addition to substrate binding to the hatch domain, three common loops of the barrel participate in substrate binding: loop 3 (BtuB, FhuA), loop 4 (BtuB, FhuA, FecA) and loop 8 (FhuA, FecA). Residues in some of the β-strands connected by these loops also participate in binding.

TBDT Structures Possess Conserved Interaction Motifs in Hatch and Barrel Domains

The barrel structures are different in their diameters and in their perimeter shapes. The barrels do not align well, and the extracellular loops show almost no structural conservation. Strands β1–β8 have essentially no sequence conservation. Barrel strands β9–β22 show some conservation localized at the hatch–barrel interface contact sites. Table II lists 12 strongly conserved residues in β9–β18. Most of these residues are involved in conserved interactions to the hatch domain.

A prominent structural feature of the β-barrel occurs beginning at strands β12 and β13. Loops 7 and 8 fold in towards the barrel lumen. These inward-folding loops

TABLE I. Structural Conservation of the Hatch Domain

Structure motif	Sequence	BtuB	FepA	FhuA	FecA
Ton box	DTLxxTAN	6–12	12–18	7–13	80–86
TEE	TxEE	30–33	32–35	54–57	108–111
PGV box	PGV	50–52	53–55	74–76	128–130
SB1 Gly	G	58	64	82	139
IRG box	IRG	68–70	74–76	92–94	149–151
LIDG box	LIDG	79–82	85–88	105–108	163–166
RP box	RxEφφRGP	106–113	121–128	128–135	191–198
latch	xYG	117–119	132–134	139–141	202–204
Hβ4	GGVVNxxT	124–131	139–146	146–153	209–216

x = non-conserved, φ = hydrophobic

TABLE II. Structural Conservation of the Barrel Domain

β-Barrel Strand or Loop	BtuB	FepA	FhuA	FecA	Hatch Interactions
9 in	D316	D368	D379	R409	Latch
10 in	Y341	F413	Y435	Y450	Latch
11 in	R358	R431	R452	R467	Latch
11 in	D360	D433	D454	E469	Latch
12 out	T370	S441	T477	L492	Latch
13 in	S392	A465	S499	S514	Latch
13 out	Y393	Y466	F500	F515	Latch
13 in	K394	K467	E501	G516	Latch
14 in	*E419*	*E511*	*E522*	*E541*	IRG box
15 in	Y436	F528	Y541	F558	IRG box
16 in	*E465*	*E567*	*E571*	*E587*	RP box
18 in	S480	N583	S587	S609	PGV box
L11	NLFD (567–570)	NLFD (677–680)	NLFD (682–685)	NIFD (707–710)	-

in = faces towards barrel lumen; out = faces towards membrane; *italics* = forms salt bridge

comprise a structural motif, which we denote the 'β-cantilever,' that breaks the regular inter-strand hydrogen bonding between β12 and β13. The β-cantilever interacts with another conserved structural motif, the 'latch' (Table I), that is located in the hatch domain. The latch motif connects hβ3 to hβ4 (Fig. 6) and is flanked on each end by highly conserved glycines (Fig. 2). Strands β9–β12 and the β-cantilever form extensive interactions with the latch. The latch motif faces strands β9–β12, fitting into a groove formed by an inward-facing tyrosine or phenylalanine residue in β10, an invariant arginine from β11, a partially conserved threonine from β12, and three sequential residues from β13. A conserved aspartate in β9 forms hydrogen bonds to the latch motif through a conserved water (BtuB, FepA, and FhuA) or directly (FecA).

Analysis of Hatch–Barrel Interfaces of TBDTs

Protein–protein interfaces can occur between individual protein subunits or between individual domains of a single protein. A vast literature (reviewed recently[42]) exists on the characterization, classification, and analysis of protein–protein interfaces. Studies of protein interfaces classify different protein–protein interactions into groups based on activity,[43] or classify the biological function of the protein interaction as homo/hetero-oligomeric, non-obligate/obligate, and transient/permanent.[31,44] In obligate protein complexes (i.e., DNA-binding protein complexes) individual protomers are active only in the protein complex and are generally not observed as individual structures.[42,45] Non-obligate complexes (i.e., signaling proteins and antigen–antibody complexes) are independently stable and can be functional in either monomeric or complex forms. Protein–protein interactions can be further defined as permanent or transient complexes. Permanent complexes are defined by long lifetime interaction, while transient complexes can form and dissociate repeatedly during their functional cycles.[44] Additional structural characterization includes calculation of the interfacial area,[46] complementarity of the fit between protein surfaces,[30] and chemical properties (polar/non-polar/hydrophobic) of residues at the interface.[47,48] The dynamic physiological conditions of cells play a role in regulation of protein interactions. The pH, ionic strength, and local protein concentration can cause dramatic shifts in specific protein interactions.[42] Current data indicate that the TBDT interface is obligate, as the hatch and barrel domains are not found in vivo as independent stable domains. We analyzed the hatch–barrel interfaces of TBDT structures in order to infer aspects of a functional mechanism by comparison to interfaces of known protein complexes.

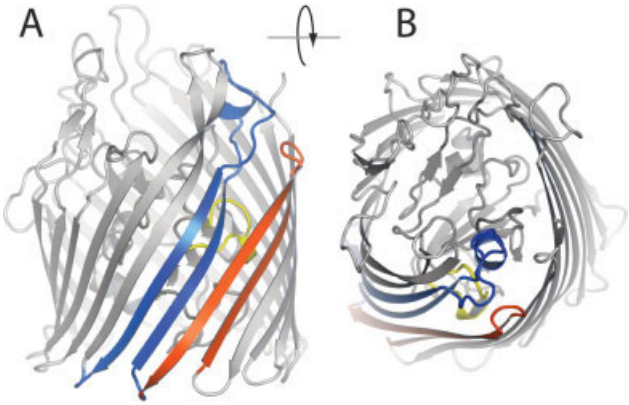

Fig. 6. The β-cantilever and latch motif in BtuB. (**A**) View from the membrane. (**B**) View from the extracellular side. The β-cantilever and β-strands 13 and 14 are shown in blue, and the latch motif is shown in yellow. The β-cantilever tilts inward and away from β-strands 11 and 12 (strands shown in red). The latch makes van der Waals contacts and conserved hydrogen bonds to the β-cantilever (not shown).

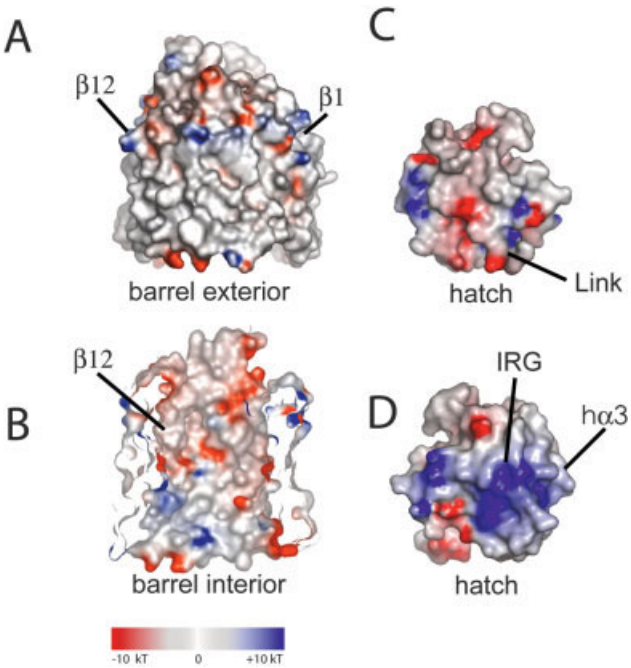

Fig. 7. Electrostatic surface potential of BtuB. Distinct locations of the barrel and hatch are annotated for orientation.

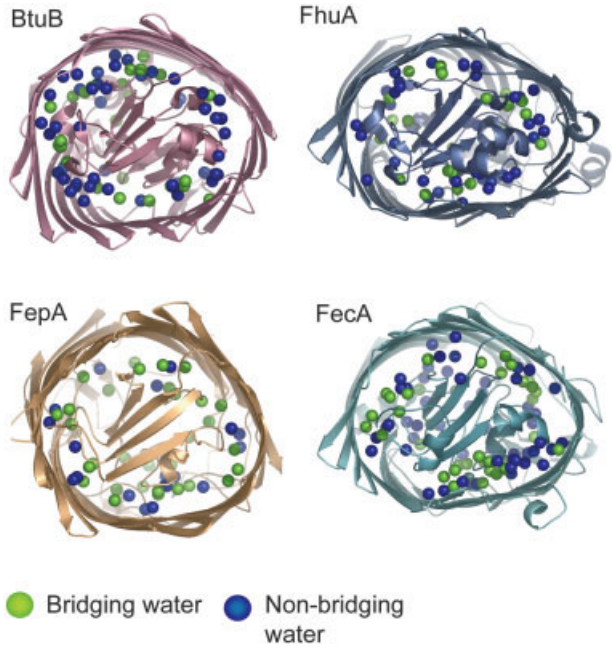

Fig. 8. Bridging and non-bridging waters at the hatch–barrel interface of TonB-dependent transporters. The structures of BtuB, FepA, FhuA, FecA are labeled. Waters are colored according to hydrogen bond type. Bridging water molecules (green) make hydrogen bonds to the hatch and barrel domains. Non-bridging water molecules (blue) reside within the interfacial region but make a hydrogen bond to only a single domain or are in extended water networks.

Fig. 9. Maltose-specific porin of *E. coli* (one monomer of the trimer is shown). The L3 loop (shown in red) folds inward and forms a selectivity filter that is necessary to restrict the flow of molecules through the porin.

Hatch–Barrel Interface Areas of TBDTs Are Large

Properties of the hatch-barrel interfaces of BtuB, FepA, FhuA, and FecA are shown in Tables III and IV. TBDT interfaces are very large and contain large numbers of hydrogen bonds and interfacial water molecules. In vivo, TBDTs are in a stable complex, but in our analyses the domains were treated as independent domains to determine their individual surface areas. The average interfacial accessible surface area (ΔASA) is 4436 ± 474 Å^2 but varies considerably among individual TBDTs. The ΔASA is largest in FhuA (4849 Å^2) and smallest in BtuB (3780 Å^2).

Hatch and Barrel Domains of TBDTs Are Well Packed

The fit of the hatch surface to the barrel surface was evaluated by calculating the gap index and shape complementarity. Specifically, gap index measures overall surface separation,[31] and the shape correlation statistic S_c measures the overall surface complementarity of the proximal atoms between the hatch and barrel domains.[30] The average gap volume, 14625 ± 2639 Å^2, is very large; much of the hatch is not in van der Waals contact with the barrel. Gap index, the ratio of gap volume to ΔASA, is 1.7 ± 0.4; this value is indicative of good overall packing. On average, the domain surfaces of TBDTs complement moderately better than the average protein–protein interface (gap index = 2). The average S_c value for TBDTs is 0.67 ± 0.05. Previous studies of shape complementarity deter-

TABLE III. Properties of TBDTs and TBDT Hatch and Barrel Domains

Property	BtuB–1NQE (2.0 Å)	FepA–1FEP (2.4 Å)	FhuA–1QFG (2.5 Å)	FecA–1KMO (2.0 Å)	Mean (SD)
Helix (%)*	12	20	13	11	14 (4)
β-sheet (%)*	28	21	22	17	22 (5)
Coil/other (%)*	60	59	65	72	64 (6)
Hatch ΔASA (Å^2)	4015	4881	5174	4816	4722 (496)
Barrel ΔASA (Å^2)	3549	4281	4524	4120	4119 (414)
Avg. ΔASA (Å^2)	3782	4581	4849	4468	4420 (454)
Total waters/hatch-associated waters	235/118	214/76	223/85	251/127	231 (16)/102 (25)
Interfacial waters	80	53	70	97	75 (18)
Non-bridging waters	50	22	49	59	45 (16)
Bridging waters	30	31	21	38	30 (7)
Total interfacial H-bonds	84	96	86	116	96 (15)
B–H hydrogen bonds	42	48	54	65	52 (10)
B-water-H hydrogen bonds	42	48	22	51	41 (13)

* = calculated by PROMOTIF[63]
ΔASA = average interfacial accessible surface area; B = barrel; H = hatch

TABLE IV. Properties of TBDT Hatch–Barrel Interfaces

Interface Parameter	BtuB	FepA	FhuA	FecA	Mean (SD)
Mean ΔASA (Å^2)	3782	4581	4911	4468	4436 (474)
Gap volume (Å^3)	14510	18388	12982	12621	14625 (2639)
Gap index (Å)	1.9	2.0	1.3	1.4	1.7 (0.4)
Shape correlation	0.65	0.61	0.69	0.72	0.67 (0.05)
Polar atoms at interface (%)	42.2	42.3	37.3	39.5	40.3 (2.4)
Salt bridges	4	2	0	4	2.5 (1.9)
Hydrogen bonds/100 Å^2	1.1	1.0	1.1	1.5	1.2 (0.22)
Bridging waters/100 Å^2	0.98	0.67	0.42	0.85	0.73 (0.24)
Interfacial waters/100 Å^2	2.2	1.2	1.4	2.2	1.8 (0.5)

mined that S_c values below 0.6 are typical of weaker interfaces, while S_c values greater than 0.7 are observed for stronger protein–protein interactions.[30]

Electrostatic Surface Properties Are Similar in TBDT Domains, and Few Salt Bridges Are Present

Highly conserved charged residues in the hatch are evident (Table II), but the electrostatic surface potential map does not possess large intensity features. The distribution of charged residues on the surface of the hatch is asymmetric. One half is neutral with several acidic residues, and the other half is neutral with several basic residues on its surface (Fig. 7). Similar to the hatch domains, the barrel domains show a principally neutral luminal surface with small regions of negative potential and neutral exterior surface (Fig. 7). The acidic surface of the hatch complements the basic interior surface of the strands β20–β6. The basic patch of the hatch also complements barrel strands β15–β17. Electrostatic analysis of the substrate-bound structures of FhuA, FecA, and BtuB does not reveal any significant differences in the interfacial region compared to the corresponding substrate-free structures. The region of the hatch near the Ton-box shows an increased negative potential following substrate binding.

The average fraction of polar atoms at the TBDT interface is 40.3% and ranges from 37.3 to 42.3% for the four proteins. Between zero and four salt bridges are observed between the hatch and barrel domains for each TBDT structure. In some instances, multiple like-charge groups are in close proximity [Fig. 5(b)]. Interactions of this type can occur in protein interfaces, where charges are distributed among several atoms but do not form stable salt bridges.[47]

Water Molecules in Hatch–Barrel Interface Form Inter-Domain Hydrogen Bonds and Solvate Individual Domains

The structures of TBDTs show waters located on the barrel interior and exterior walls, as well as on all sides of the hatch. We limited our analysis to interfacial waters, those waters associated with the hatch–barrel interface. We distinguish between two classes of interfacial water molecules located in the hatch-barrel interface, *bridging waters*, and *non-bridging waters*. *Bridging waters* participate in inter-domain hydrogen bond formation. *Non-bridging waters* are within 3.5 Å of both domains of the interface but only form hydrogen bonds to either the hatch or the barrel. The resolution of the structures used in this analysis ranges from 2.0 to 2.7 Å, with three structures at resolutions higher than 2.7 Å, permitting some confidence in the positions (and existence) of waters in these refined structures.

Approximately 75 ± 18 crystallographic waters reside in the interfacial region between the hatch and barrel domains (Table III, Fig. 6). About two-thirds of these interfa-

cial waters are hydrogen bonded to either the hatch or the barrel or are involved in water networks (Fig. 8). About one-third of the interfacial waters form bridging hydrogen bonds to both domains in the interface. The fraction of interfacial waters that are bridging waters for TBDTs is in the low range of proteins examined. There is an average of 3.1 hydrogen bonds per water across the domain interface.

There are approximately 95 hydrogen bonds across the TBDT hatch–barrel interface. We divided the interfacial hydrogen bonds into two categories: protein–protein for those between the hatch and barrel, or protein–water–protein for those that use water as a hydrogen-bond bridge between the domains. The ratio of protein–protein (52) to protein–water–protein (47) hydrogen bonds is 1.1 (Table IV). Thus, nearly 50% of the interfacial hydrogen bonds are formed through bridging waters (Fig. 8). There is an even distribution of waters in the interface; i.e., the interfacial region appears rather uniformly hydrated. Noncontacting areas or gaps in the interface are filled by water networks. With the exception of FhuA, water mediates about 50% of the interfacial hydrogen bonds. This is indicative of a poorly packed surface that requires many waters to act as intermediates for the otherwise poor hydrogen bonding geometry across the interface.[43,47]

Discussion

In our analysis, we have used structural alignment coupled to sequence alignment to identify strongly conserved regions in TBDTs that are likely to be important for function. The majority of conserved residues in TBDT occur at positions within the hatch–barrel interface. Additionally we have analyzed the interface between the hatch and barrel domains. Our analysis indicates that the TBDT hatch–barrel interface is transient and that the hatch domain can undergo significant rigid-body movement and/or conformational fluctuation within the barrel during the transport cycle. Interfacial properties and experimental evidence lend support to this hypothesis. Water plays a major role in the formation of the domain interface and likely mitigates the energetic cost of hatch movement and conformational change within the barrel during transport. We hypothesize that the strongly conserved latch and β-cantilever structural motifs play a major role in the transport cycle and that during the transport cycle the hatch moves and unfolds from within the barrel.

Conserved Structural Motifs Position Substrate-Binding Loops (Apices) of the Hatch Within the Barrel Domain

Multiple-species alignment of TBDTs shows the invariant conservation of the PGV and IRG tri-peptides (data not shown). These sequences flank the substrate binding loops of the hatch and make interactions to the barrel. We propose that these interactions, which include the conserved charge cluster, are not critical for stabilizing the hatch with the barrel but rather are important for proper folding of the SB1 and SB2 loops. We hypothesize that the positively charged electrostatic surface of the IRG/RP motif guides the hatch into position through electrostatic interaction with the two glutamates of β14 and β16; a similar idea was previously stated in an analysis of the FepA crystal structure.[19] The SB1 loop position is constrained by its flanking PGV and IRG sequences. The IRG motif is 'pinned' to the barrel wall at strands β14–β16. The PGV motif forms three backbone hydrogen bonds to the IRG motif, forcing the SB1 loop to extend toward β3 and β4. The SB1 loops can accommodate different substrates of individual TBDTs through variability at residues distal to the PGV/IRG motifs. Like SB1, the SB2 position is also coupled to the IRG motif, constraining the SB2 position in the center of the extracellular lumen. The overall positioning of the hatch binding loops (apices) is critical because they act in concert with loops from the barrel for high affinity substrate binding.[18–22,49–51] Although the extracellular loops of the barrel are poorly conserved, substrate binding is achieved through extracellular loop residues at similar spatial locations. Nearby 'spatially conserved' residues from the barrel strands and loops of BtuB, FhuA, and FecA all undergo conformational shift to bind their respective substrates. Thus, to achieve proper substrate binding, the loops and barrel strands must be correctly positioned relative to one another.

β-Cantilever May Function to Occlude Barrel Lumen During Transport Cycle

The β-cantilever (β13–β15) is resting in an upright conformation in intimate contact with the latch motif of the hatch, leaving the lumen open to the extracellular millieu. This interaction between the β-cantilever and the latch motif may be important to stabilize the β-cantilever in its open conformation. The β-cantilevers of FhuA, FecA, and BtuB exhibit different conformational changes upon substrate binding. In BtuB the β-cantilever undergoes nearly no conformational change and remains upright, making minimal contact with cyanocobalamin.[34] In FhuA, the β-cantilever moves slightly towards the lumen to interact with the ferrichrome.[12] In FecA, the β-cantilever moves into the upper lumen to cover the ferric dicitrate.[20,21] The β-cantilever of BtuB is sterically restricted by the large cyanocobalamin substrate and cannot move. Ferrichrome, the substrate of FhuA, is about the half the size of cyanocobalamin; thus, the FhuA β-cantilever can make small movements towards its substrate. Ferric dicitrate, the substrate of FecA, is considerably smaller; thus, the FecA β-cantilever can undergo significant conformational changes to cover the substrate. We hypothesize that during the transport cycle, the β-cantilever of TBDTs follows a conformational trajectory of initial extension away from the barrel, movement towards the lumen of the barrel, and, finally, folding into the lumen of the barrel. A portion of this trajectory, different positions of the folding of the β-cantilever, is seen in the range of its position due to variable substrate size in the substrate-bound structures of BtuB, FhuA and FecA.

Interestingly, the β-cantilever is a structural feature similar to the specificity loop L3 of general diffusion porins (OmpC, OmpF, PhoE) and the specific diffusion porins (LamB, ScrY). The loop is folded into the barrel and

constricts the cross section of the porin. The β-cantilever conformation is most similar to that of L3 of LamB and ScrY. In LamB and ScrY, β5 diverges away from β4 (Fig. 9) and β5/β6 together with L3 fold inward to form the pore-occluding loop.[52,53] In TBDTs, the β-cantilever may move into a similar position to occlude the pore at some step of the transport cycle. Such a conformational change would be supportive of an hypothesized 'close before opening' mechanism of TBDT function.[54] The conformation of the hatch domain within the barrel is likely to change during the transport cycle. These conformational changes could include distortion of the hatch within the barrel to open up a substrate permeation pathway, partial or complete exit of the hatch from the barrel, or a combination of these structural changes. Exit of the hatch from the barrel could create a hole across the outer membrane of approximately 35–40 Å in diameter. The toxic effects of a hole that could pass macromolecules/solutes of mass up to 20000 Da[55] would be prevented by the β-cantilever folding down to block this large pore. Deletion of the extracellular loop adjacent to the β-cantilever in TBDTs or porins causes a wide range of phenotypic changes. In FepA, deletion of this loop abrogates substrate binding and transport, and destabilizes the protein.[56] In BtuB, deletion of this loop changes transport specificity and permits the uptake of ferrichrome in a *fhua* host strain.[57] In OmpF, antibiotic sensitivity increases;[58] in LamB, the native protein structure is destabilized.[59]

The Hatch–Barrel Interface Resembles Those Found in Transient Protein Complexes

Our analysis indicates that the hatch–barrel interface of TBDTs has characteristics that are similar to those observed in transient protein complexes that undergo conformational change and/or domain movement during their function. The TBDT shape correlation compares well to typical antigen–antibody interactions (S_c = 0.6-0.7), and further comparison shows that the TBDT interface S_c value is below the expected value for an obligate homodimer (S_c = 0.7-0.8).[30] The average gap index (1.8) of the hatch–barrel interfaces of TBDTs is close to the gap index of monomeric protein interfaces (1.9), indicative of a normal domain–domain interaction. Transient complexes contain more hydrophilic residues in their interfaces than permanent complexes and contain a larger proportion of charged groups.[43,45] The hatch–barrel interfaces contain approximately 40% polar residues, consistent with the fraction seen in transient complex interfaces.[43,48]

Water Molecules in Hatch–Barrel Interfaces of TBDTs Can Reduce the Activation Energy of the Transport Cycle

Among the four TBDT structures, there is an average of approximately 75 crystallographic waters present within the hatch–barrel interface (Table III). The number of hydrogen bonds per 100 Å^2 in TBDTs (1.2 ± 0.2) is greater than that in the average protein–protein interaction (0.8).[43,45,47] Comparison to the interfaces of known permanent and transient protein–protein interactions shows that permanent complexes have 0.7 hydrogen bonds per 100 Å^2, while transient complexes have 1.1 hydrogen bonds per 100 Å^2.[45] This suggests, based on the number of interfacial hydrogen bonds, that the TBDT interface has properties similar to that of a transient protein interaction. In our analysis of interfacial waters, we classify interfacial waters as bridging waters that form hydrogen bonds to both the hatch and barrel domains or non-bridging waters that solvate one of the domains. Strikingly, only approximately one-third of the interfacial waters are bridging waters, a fraction lower than is typical. Thus, the majority of interfacial waters directly solvate either the hatch or barrel domains, or are in more extended water networks. Specifically, in the TBDT structures analyzed, approximately 80% of these 'non-bridging' waters are equally divided between solvating the hatch and barrel domains and participating in water networks (data not shown). The average number of hydrogen bonds per water molecule, 3.1, is lower than the value of 3.8 that is typical for interfacial waters.[47] These two features, a low fraction of bridging waters at the hatch–barrel interfaces and an average of approximately three hydrogen bonds per water molecule, strongly suggest a view of the hatch domain as being solvated within the barrel with excess water molecules and excess hydrogen-binding capacity available to facilitate hatch movement and/or conformational change during the transport cycle. This water bushing could greatly reduce the energetic cost associated with perturbations of the hatch–barrel interface that would accompany hatch conformational change, unfolding, or movement. A fluctuating water network with hydrogen bonds being broken and re-formed with little net energy change (not unlike the fluctuating hydrogen bonds in liquid water) is compatible with the analysis of waters built into the four independently determined TBDT structures. A similar statement about the 'lubricating effect' of waters in the hatch–barrel interface lowering the activation energy for transport was made in a recent analysis of molecular dynamics simulations of FhuA.[60]

Single-Molecule Unfolding Experiments Suggest a Possible Mechanistic Step in the TBDT Active Transport Cycle

How does TonB interact with TBDTs to facilitate active transport? One possibility is that the binding of TonB to the transporter drives a conformational change and/or movement in the hatch domain. Recent experiments in single-molecule unfolding suggest that only modest mechanical forces may be required to affect substantial conformational change in a protein or protein domain.[61,62] The key finding of these experiments is that the force required to unfold a protein can depend critically upon the direction at which that pulling force is applied. Both studies were performed on β-sheet proteins. The orientation of the pulling force with respect to these proteins can be described as either 'parallel' or 'perpendicular.' A parallel direction of applied pulling force is roughly parallel to β-strand orientation, requiring the simultaneous breaking of multiple interstrand hydrogen bonds to unfold the

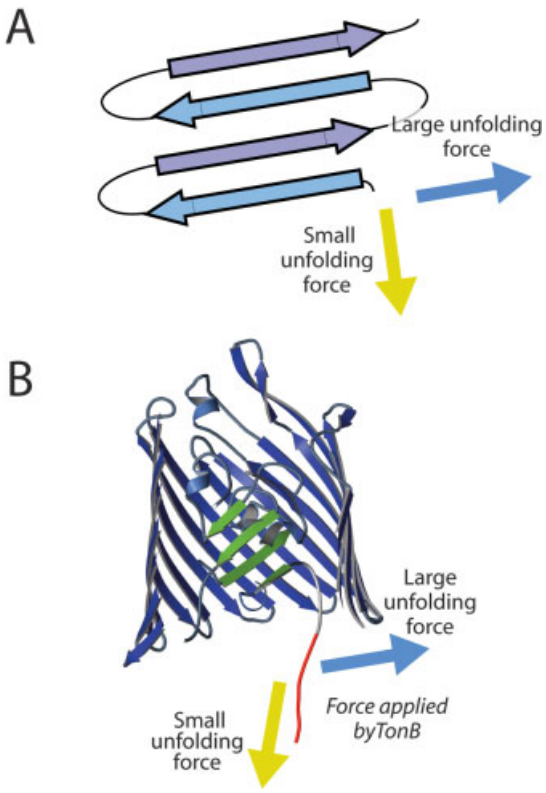

Fig. 10. Mechanical unfolding of the hatch domain as a possible step in the TonB-dependent outer membrane active transport cycle. (**A**) Single-molecule force spectroscopy experiments indicate that the direction of an applied unfolding force dramatically affects the amount of force required to unfold a β-sheet protein domain. (**B**) The conserved core of the hatch domains of TBDTs is a four-stranded β-sheet. As shown in this cutaway view, the strands of the sheet (green) are approximately parallel to the periplasmic opening of the barrel. TonB interacts with TBDTs at this periplasmic surface. If this interaction leads to TonB applying a mechanical pulling force, the direction of this applied force could drive substantial unfolding or conformational change of the hatch domain.

protein. A perpendicular direction will rupture hydrogen bonds sequentially, 'unzipping' β-strands. This difference in direction is manifested as an anisotropy of forces required to unfold β-sheet proteins. In ubiquitin, a four-stranded twisted β-sheet, two different parallel orientations of pulling force were achieved.[62] One orientation ruptured five hydrogen bonds between a pair of parallel β-strands, and the other orientation ruptured five hydrogen bonds between a different pair of anti-parallel β-strands. This seemingly modest difference yielded unfolding forces of 203 ± 35 pN (at 400 nm/s) for the parallel β-strands versus 85 ± 20 pN (at 300 nm/s) for the anti-parallel β-strands. The results are even more striking for experiments performed with E2lip3, a lipoyl domain from a subunit of the pyruvate dehydrogenase multienzyme complex.[61] E2lip3 consists of two four-stranded β-sheets. A parallel force of 177 ± 3 pN (at 700 nm/s) unfolded this protein. By contrast, the perpendicular force required to unfold E2lip3 was not measurable, less than 15 pN.

The force required to unfold a protein can vary by more than an order of magnitude. For β-sheet proteins, application of a very modest perpendicular force may be sufficient to drive an unfolding event. The hatch domain of TBDTs is a core four-stranded β-sheet. In any of these structures, application of a force on the hatch by TonB would be perpendicular in orientation (Fig. 10). Therefore, we speculate that a very modest mechanical force applied by TonB when it couples to the hatch domain of a TBDT could be sufficient to cause substantial conformational change or unfolding of the hatch. Clearly, this hypothesis awaits further testing by experiment and computation.

CONCLUSIONS

Detailed analysis of the four extant TBDT crystal structures indicates conserved structural elements that are likely important for function (rather than for substrate recognition). Analysis of the hatch–barrel interfaces of TBDTs indicates a similarity in properties to transient protein complex interfaces. Significantly, most of the interfacial waters solvate the hatch or barrel domains rather than participating in bridging hydrogen bond formation between the hatch and the barrel. These solvating waters can function as a lubricant to reduce the energetic cost of movement of the hatch within the barrel. Lastly, an examination of recent single-molecule unfolding experiments in the context of TBDTs suggests that a very modest mechanical force by TonB upon the transporter could drive large conformational changes or unfolding of the hatch domain during the active transport cycle.

REFERENCES

1. Nikaido H. Molecular basis of bacterial outer membrane permeability revisited. Micro Mol Biol Rev 2003;67:593–656.
2. Higgs PI, Myers PS, Postle K. Interactions in the TonB-dependent energy transduction complex: ExbB and ExbD form homomultimers. J Bacteriology 1998;180:6031–6038.
3. Larsen RA, Thomas MG, Postle K. Protonmotive force, ExbB and ligand-bound FepA drive conformational changes in TonB. Mol Micro 1999;31:1809–1824.
4. Bell PE, Nau CD, Brown JT, Konisky J, Kadner RJ. Genetic suppression demonstrates interaction of TonB protein with outer membrane transport proteins in *Escherichia coli*. J Bacteriol 1990;172:3826–3829.
5. Postle K. TonB protein and energy transduction between membranes. J Bioenerg and Biomem 1993;25:591–601.
6. Lundrigan MD, Kadner RJ. Nucleotide sequence of the gene for the ferrienterochelin receptor FepA in *Escherichia coli*. Homology among outer membrane receptors that interact with TonB. J Biol Chem 1986;261:10797–10801.
7. Schramm E, Mende J, Braun V, Kamp RM. Nucleotide sequence of the colicin B activity gene *cba*: consensus pentapeptide among TonB-dependent colicins and receptors. J Bacteriol 1987;169:3350–3357.
8. Larsen RA, Foster-Hartnett D, McIntosh MA, Postle K. Regions of *Escherichia coli* TonB and FepA proteins essential for *in vivo* physical interactions. J Bacteriol 1997;179:3213–3221.
9. Cadieux N, Phan PG, Cafiso DS, Kadner RJ. Differential substrate induced signalling through the Ton-B dependent transporter BtuB. Proc Natl Acad Sci USA 2003;100:10688–10693.
10. Cadieux N, Kadner RJ. Site-directed disulfide bonding reveals an interaction site between energy-coupling protein TonB and BtuB, the outer membrane cobalamin transporter. Proc Natl Acad Sci USA 1999;96:10673–10678.
11. Merianos HJ, Cadieux N, Lin CH, Kadner RJ, Cafiso DS. Substrate-induced exposure of an energy-coupling motif of a membrane transporter. Nat Struct Biol 2000;7:205–209.
12. Ferguson AD, Hofmann E, Coulton JW, Diederichs K, Welte W. Siderophore-mediated iron transport: crystal structure of FhuA with bound lipopolysaccharide. Science 1998;282:2215–2220.

13. Ogierman M, Braun V. Interactions between the outer membrane ferric citrate transporter FecA and TonB: studies of the FecA TonB box. J Bacteriol 2003;185:1870–1885.
14. Khursigara C, Crescenzo G, Pawlek P, Coulton JW. Enhanced binding of TonB to a ligand-loaded outer membrane receptor. J Biol Chem 2004;279:7405–7412.
15. Koedding J, Howard P, Kaufmann L, Polzer P, Lustig A, Welte W. Dimerization of TonB is not essential for its binding to the outer membrane siderophore receptor FhuA of *Escherichia coli*. J Biol Chem 2004;279:9978–9986.
16. Chang C, Mooser A, Pluckthun A, Wlodawer A. Crystal structure of the dimeric C-terminal domain of TonB reveals a novel fold. J Biol Chem 2001;276:27535–27540.
17. Ghosh J, Postle K. Evidence for dynamic clustering of carboxy-terminal aromatic amino acids in TonB-dependent energy transduction. Mol Micro 2004;51:203–213.
18. Locher KP, Rees B, Koebnik R, Mitschler A, Moulinier L, Rosenbusch JP, Moras D. Transmembrane signaling across the ligand-gated FhuA receptor: crystal structures of free and ferrichrome-bound states reveal allosteric changes. Cell 1998;95:771–778.
19. Buchanan SK, Smith BS, Venkatramani L, Xia D, Esser L, Palnitkar M, Chakraborty R, van der Helm D, Deisenhofer J. Crystal structure of the outer membrane active transporter FepA from *Escherichia coli*. Nat Struct Biol 1999;6:56–63.
20. Ferguson AD, Chakraborty R, Smith BS, Esser L, van der Helm D, Deisenhofer J. Structural basis of gating by the outer membrane transporter FecA. Science 2002;295:1715–1719.
21. Yue WW, Grizot S, Buchanan SK. Structural evidence for iron-free citrate and ferric citrate binding to the TonB-dependent outer membrane transporter FecA. J Mol Biol 2003;332:353–368.
22. Chimento DP, Mohanty AK, Kadner RJ, Wiener MC. Substrate induced transmembrane signalling in the cobalamin transporter BtuB. Nat Struct Biol 2003;10:394–401.
23. Szustakowski JD, Weng Z. Protein structure alignment using a genetic algorithm. Proteins 2000;38:428–440.
24. Aiyar A. The use of CLUSTAL W and CLUSTAL X for multiple sequence alignment. Meth Mol Bio 2000;132:221–241.
25. Hall TA. BioEdit: a user-friendly biological sequence alignment editor and analysis program for Windows 95/98/NT. Nucl Acids Symp Series 1999;41:95–98.
26. Wallace AC, Laskowski RA, Thornton JM. LIGPLOT: a program to generate schematic diagrams of protein-ligand interactions. Prot Eng 1995;8:127–134.
27. Thornton JM, Edwards MS, Taylor WR, Barlow DJ. Location of 'continuous' antigenic determinants in the protruding regions of proteins. EMBO Journal 1986;5:409–413.
28. Creighton T. Proteins: structures and molecular properties. New York: W.H. Freeman; 1993.
29. Nicholls A, Sharp KA, Honig B. Protein folding and association: insights from the interfacial and thermodynamic properties of hydrocarbons. Proteins 1991;11:281–296.
30. Lawerence M, Colman P. Shape complementarity at protein/protein interfaces. J Mol Biol 1993;234:946.
31. Jones S, Thornton JM. Principles of protein–protein interactions. Proc Natl Acad Sci USA 1996;93:13–20.
32. DeLano WL. The Pymol Molecular Graphics System. San Carlos, CA: DeLano Scientific; 2002.
33. Braun V. Surface signaling: novel transcription initiation mechanism starting from the cell surface. Arch Microbiol 1997;167:325–331.
34. Chimento DP, Kadner RJ, Wiener MC. The *Escherichia coli* outer membrane cobalamin transporter BtuB: structural analysis of calcium and substrate binding, and identification of orthologous transporters by sequence/structure conservation. J Mol Biol 2003;332:999–1014.
35. Endriβ F, Braun M, Killmann H, Braun V. Mutant analysis of the *Escherichia coli* FhuA protein reveals sites of FhuA activity. J Bacteriol 2003;185:4683–4692.
36. Fanucci GE, Cadieux N, Piedmont CA, Kadner RJ, Cafiso DS. Structure and dynamics of the beta-barrel of the membrane transporter BtuB by site-directed spin labeling. Biochemistry 2002;41:11543–11551.
37. Fanucci GE, Cafiso DS. Spectroscopic evidence that osmolytes used in crystallization buffers inhibit a conformation change in a membrane protein. Biochemistry 2003;42:13106–13112.
38. Chimento DP, Mohanty AK, Kadner RJ, Wiener MC. Crystallization and initial X-ray diffraction of BtuB, the integral membrane cobalamin transporter of *Escherichia coli*. Acta Cryst D 2003;59:509–511.
39. Pressler U, Staudenmaier H, Zimmermann L, Braun V. Genetics of the iron dicitrate transport system of *Escherichia coli*. J Bacteriol 1988;170:2716–2724.
40. Barnard TJ, Watson jr ME, McIntosh MA. Mutations in the *Escherichia coli* receptor FepA reveal residues involved in ligand binding and transport. Mol Micro 2001;41:527–536.
41. Chakraborty R, Lemke EA, Cao Z, Klebba PE, van der Helm D. Identification and mutational studies of conserved amino acids in the outer membrane receptor protein, FepA, which affect transport but not binding of ferric-enterobactin in *Escherichia coli*. Biometals 2003;16:507–518.
42. Nooren IM, Thornton JM. Diversity of protein-protein interactions. EMBO Journal 2003;22:3486–3492.
43. Lo Conte L, Chothia C, Janin J. The atomic structure of protein-protein recognition sites. J Mol Biol 1999;285:2177–2198.
44. Nooren IM, Thornton JM. Structural characterization and functional significance of transient protein-protein interactions. J Mol Biol 2003;325:991–1018.
45. Jones S, Marin A, Thornton JM. Protein domain interfaces: characterization and comparison with oligomeric protein interfaces. Prot Eng 2000;13:77–82.
46. Miller S, Lesk AM, Janin J, Chothia C. The accessible surface area and stability of oligomeric proteins. Nature 1987;328:834–836.
47. Xu D, Tsai CJ, Nussinov R. Hydrogen bonds and salt bridges across protein-protein interfaces. Prot Eng 1997;10:999–1012.
48. Tsai CJ, Lin SL, Wolfson HJ, Nussinov R. Studies of protein-protein interfaces: a statistical analysis of the hydrophobic effect. Protein Sci 1997;6:53–64.
49. Ferguson AD, Braun V, Fiedler HP, Coulton JW, Diederichs K, Welte W. Crystal structure of the antibiotic albomycin in complex with the outer membrane transporter FhuA. Protein Sci 2000;9:956–963.
50. Ferguson AD, Kodding J, Walker G, Bos C, Coulton JW, Diederichs K, Braun V, Welte W. Active transport of an antibiotic rifamycin derivative by the outer-membrane protein FhuA. Structure 2001;9:707–716.
51. Ferguson AD, Deisenhofer J. TonB-dependent receptors-structural perspectives. Biochim Biophys Acta 2002;1565:318–332.
52. Schirmer T, Keller TA, Wang YF, Rosenbusch JP. Structural basis for sugar translocation through maltoporin channels at 3.1 Å resolution. Science 1995;267:512–514.
53. Forst D, Welte W, Wacker T, Diederichs K. Structure of the sucrose-specific porin ScrY from *Salmonella typhimurium* and its complex with sucrose. Nat Struct Biol 1998;5:37–46.
54. Postle K. Close before opening. Science 2002;295(5560):1658–1659.
55. Harlan J, Picot D, Loll P, Garavito R. Calibration of size-exclusion chromatography: use of a double Gaussian distribution function to describe pore sizes. Anal Biochem 1995;224:557–563.
56. Newton SM, Igo JD, Scott DC, Klebba PE. Effect of loop deletions on the binding and transport of ferric enterobactin by FepA. Mol Micro 1999;32:1153–1165.
57. Lathrop JT, Wei BY, Touchie GA, Kadner RJ. Sequences of the *Escherichia coli* BtuB protein essential for its insertion and function in the outer membrane. J Bacteriol 1995;177:6810–6819.
58. Benson SA, Occi JLL, Sampson BA. Mutations that alter the pore function of the OmpF porin of *Escherichia coli* K12. J Mol Biol 1988;203:961–970.
59. Klebba PE, Hofnung M, Charbit A. A model of maltodextrin transport through the sugar-specific porin, LamB, based on deletion analysis. EMBO J 1994;13:4670–4675.
60. Faraldo-Gomez JD, Smith GR, Sansom MSP. Molecular dynamics simulations of the bacterial outer membrane protein FhuA: a comparative study of the ferrichrome-free and bound states. Biophys J 2003;85:1406–1420.
61. Brockwell D, Paci E, Zinober R, Beddard G, Olmstead P, Smith D, Perham R, Radford S. Pulling geometry defines the mechanical resistance of a beta-sheet protein. Nat Struct Biol 2003;10:731–737.
62. Carrion-Vasquez M, Hongbin L, Lu H, Marszalek PE, Oberhauser AF, Fernandez JM. The mechanical stability of ubiquitin is linkage dependent. Nat Struct Biol 2003;10:738–743.
63. Hutchinson EG, Thornton JM. PROMOTIF—a program to identify and analyze structural motifs in proteins. Protein Science 1996;5:212–220.